

1
2
3
4
5
6
7
8
9
10
11
12
13
14
15
16

SUPPLEMENTARY MATERIAL
INCLUDING ONE TABLE AND SIX FIGURES

**European summer temperature response
to annually dated volcanic eruptions over the past nine centuries**

Jan Esper^{1,*}, Lea Schneider¹, Paul J. Krusic², Jürg Luterbacher³, Ulf Büntgen⁴, Mauri Timonen⁵,
Frank Sirocko⁶, Eduardo Zorita⁷

¹*Department of Geography, Johannes Gutenberg University, 55099 Mainz, Germany*

²*Department of Physical Geography and Quaternary Geology, Stockholm University, 10691
Stockholm, Sweden*

³*Department of Geography, Climatology, Climate Dynamics and Climate Change, Justus-Liebig
University, 35390 Giessen, Germany*

⁴*Swiss Federal Research Institute WSL, 8903 Birmensdorf, Switzerland*

⁵*Finnish Forest Research Institute, Rovaniemi Research Unit, 96301 Rovaniemi, Finland*

⁶*Institute for Geoscience, Johannes Gutenberg University, 55099 Mainz, Germany*

⁷*Institute for Coastal Research, HZG Research Centre, 21494 Geesthacht, Germany*

17 **Coupled General Circulation Models (CGCMs)**

18 Four millennium-long simulations from three CGCMs were used for assessing post-volcanic cooling
19 effects in Europe. These include two runs of the ECHO-G model (Erik1 and Erik2; Zorita et al. 2005),
20 and two simulations downloaded from the CMIP5 dataset (Taylor et al. 2012). The latter two are the
21 Max-Planck-Institute Earth System Model Paleoclimate version (MPI-ESM-P; Giorgetta et al. 2013),
22 and the Community Climate System Model version 4 (CCSM4; Gent et al. 2011). The simulations
23 retrieved from the CMIP archive cover the periods 850-1850 and 1850-2005 C.E., and were combined
24 here to produce a single continuous temperature timeseries spanning the past millennium. The two
25 ECHO-G simulations provide continuous coverage from 1000-1990 C.E. (see Fernández-Donado et
26 al. 2013 for an overview on paleo model simulations).

27 All models are coupled atmosphere-ocean models. The ECHO-G model was developed at the Max-
28 Planck-Institute for Meteorology in Hamburg and consists of the atmospheric model ECHAM4 and
29 the ocean model HOPE. ECHO-G was used, with 21 others, in the Fourth Assessment Report issued
30 by Intergovernmental Panel on Climate Change (Solomon et al. 2007) to produce future climate
31 projections. The horizontal resolution of the ECHO-G model atmosphere (3.75 x 3.75 degrees) is also
32 coarser than in the CMIP models.

33 The CMIP models used here can be considered as sophisticated climate models of the latest generation
34 and are being used for climate projections included in next IPCC Assessment Report due in 2013. The
35 MPI-ESM-P model consists of the spectral atmospheric model ECHAM6 with a horizontal resolution
36 of approximately 1.87 x 1.87 degrees. The atmosphere model is coupled to the ocean model OM. The
37 CCSM4 model was developed at the National Center for Atmospheric Research. The atmospheric
38 model is a finite-difference model with a considerably finer horizontal resolution of about 1 x 1.25
39 degrees (latitude x longitude).

40 The external climate forcings used to drive the ECHO-G and CMIP5 models differ. All simulations
41 include a representation of past solar energy output (total solar irradiance; TSI) assuming solar energy
42 varies equally at all wavelengths of the electromagnetic spectrum. All simulations essentially assume
43 the same shape of past TSI variability, derived from concentrations of the cosmogenic isotope ¹⁰Be in
44 polar ice cores, but the amplitude of the TSI variability may vary among simulations. The ECHO-G
45 simulations assume a change in TSI of 0.3% between present (1961-1990) and the Late Maunder
46 Minimum (1675-1715), whereas the CMIP models assume smaller changes of only 0.15%. Volcanic
47 forcing in the ECHO-G simulations was implemented as a simple reduction of TSI, in an attempt to
48 parameterize the effects of volcanic eruptions in a climate model with a coarsely resolved stratosphere.
49 The estimations of volcanic eruptions affect on short wave radiative forcing are based on Crowley
50 (2000). The CMIP models implement a more sophisticated volcanic forcing scheme with spatially and
51 seasonally resolved variations of atmospheric optical depth. Estimates of optical depth changes are
52 based on different datasets of acidity measures in polar ice cores. The MPI-ESM-P model uses the

53 optical depth reconstruction from Crowley (2008), the CCSM4 model used estimates from Gao et al
54 (2008).

55 The ECHO-G and CCSM4 models consider past variations of carbon dioxide and methane estimated
56 from trapped air bubbles in polar ice cores. In the MPI-ESM-P model, the concentration of carbon
57 dioxide and methane are interactively simulated by a carbon-cycle module that incorporates the
58 geochemistry of the ocean, the land biosphere and their interaction with climate.

59

60 **Supplementary Table**

61

62 **Table S1.** Long instrumental station records from Northern and Central Europe. "Period" specifies the
63 time span common to all MXD chronologies (the Lau chronology ends in 1976) and the shorter
64 (Stockholm, Berlin) and longer (Uppsala, Central England, De Bilt) station records. For station
65 locations see Fig. S1

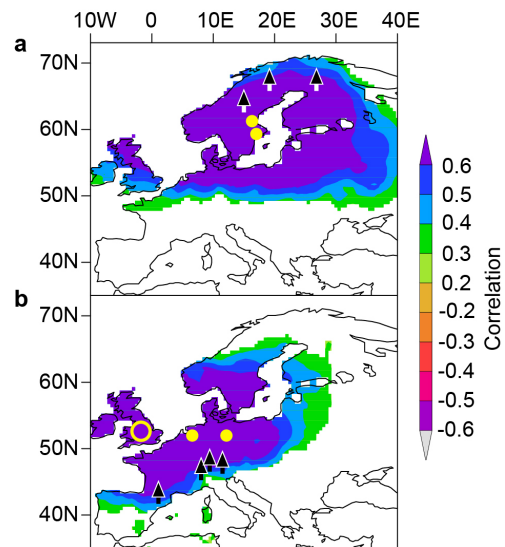
	Station	Country	Period	Source
N-Eur	Uppsala	Sweden	1722-1976	Moberg and Bergström (1997)
	Stockholm	Sweden	1756-1976	Moberg and Bergström (1997)
C-Eur	Centr. England	England	1722-1976	Manley (1974)
	De Bilt	Netherlands	1722-1976	van den Dool et al. (1978)
	Berlin	Germany	1756-1976	Vose et al. (1992)

66

67

68 **Supplementary Figures**

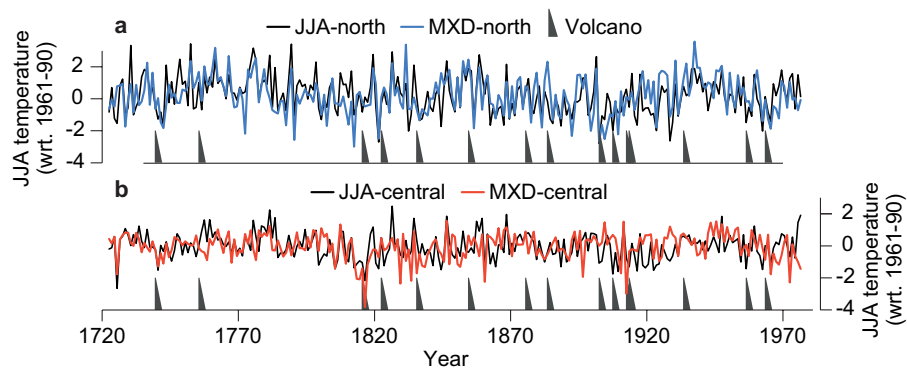
69



70

71 **Fig. S1** Spatial domains of the long instrumental station records from Northern and Central Europe. **a**
72 Correlation patterns of the mean JJA temperature of the Uppsala and Stockholm stations (yellow
73 circles) with gridded summer temperatures over the 1901-1976 period ($p < 0.01$). Black triangles are
74 the JAE, TOR, and NSC MXD sites (from west to east). **b** Same as in **a**, but for the mean timeseries of
75 the Central England, De Bilt, and Berlin stations (from west to east). Triangles are the PYR, LOE,
76 LAU, and TIR MXD sites (from west to east)

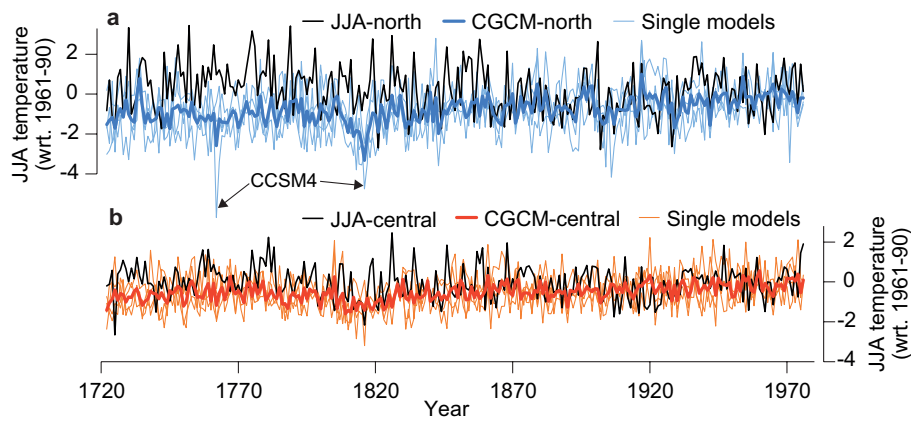
77



79

80 **Fig. S2** Summer temperature from long instrumental station and MXD records in Northern and
 81 Central Europe. **a** JJA mean temperature from the Stockholm and Uppsala stations (black; JJA-north)
 82 together with the mean MXD record of JAE, TOR, and NSC (blue; MXD-north) over their 1722-1976
 83 common period. Grey triangles indicate the 15 annually dated volcanic eruptions, $VEI \geq 5$. The MXD
 84 timeseries was scaled to the instrumental data over the 1722-1976 period. **b** Same as in **a**, but for JJA
 85 mean temperatures from Central England, De Bilt, and Berlin (JJA-central) together with the mean
 86 MXD timeseries from PYR, LAU, LOE, and TIR (MXD-central). All timeseries expressed as
 87 temperature deviations from the 1961-1990 mean

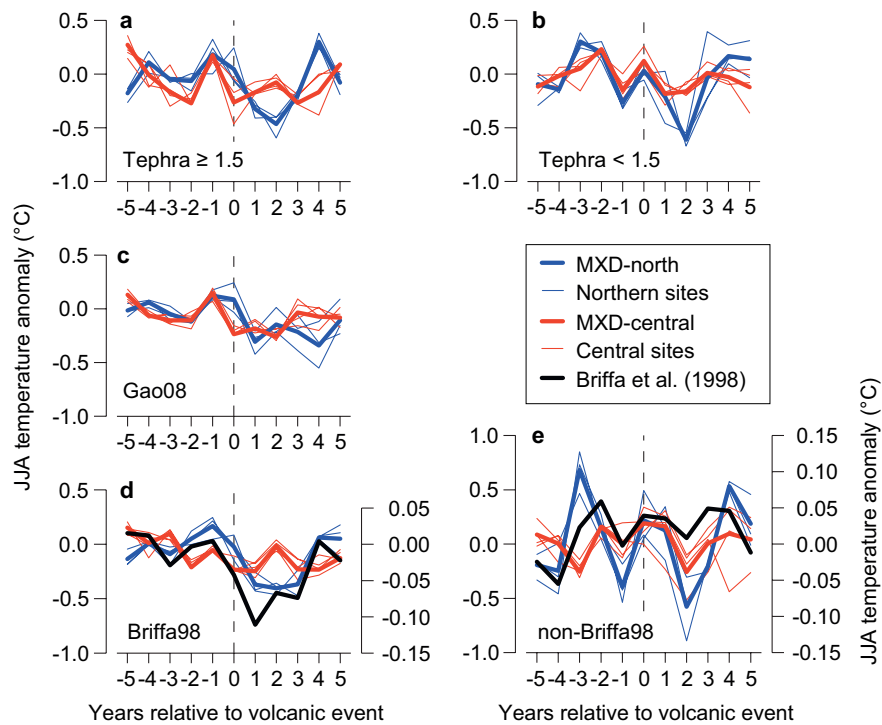
88



90

91 **Fig. S3** Summer temperature from long instrumental stations and CGCM simulations. **a** JJA mean
 92 temperature of the Stockholm and Uppsala stations (JJA-north, black) together with the arithmetic
 93 mean of four CGCM simulations (CGCM-north, blue) over their 1722-1976 common period. Single
 94 model runs (CCSM4, Erik1, Erik2, MPI-ESM-P; thin curves) represent JJA temperatures of five grid
 95 points in proximity to the meteorological stations and MXD sites in Northern Europe. Severe negative
 96 deviations of the CCSM model in 1762 and 1816 following ice core derived volcanic sulfate
 97 depositions of 8.4 Tg and 59.7 Tg (Gao et al. 2008), respectively, are labeled. **b** Same as in **a**, but for
 98 JJA mean temperatures from the Central England, De Bilt, and Berlin stations (JJA-Central) together
 99 with the CGCM timeseries integrating summer temperatures at seven grid points in proximity to the
 100 station and MXD sites in Central Europe. All temperatures expressed as anomalies with respect to the
 101 1961-1990 mean

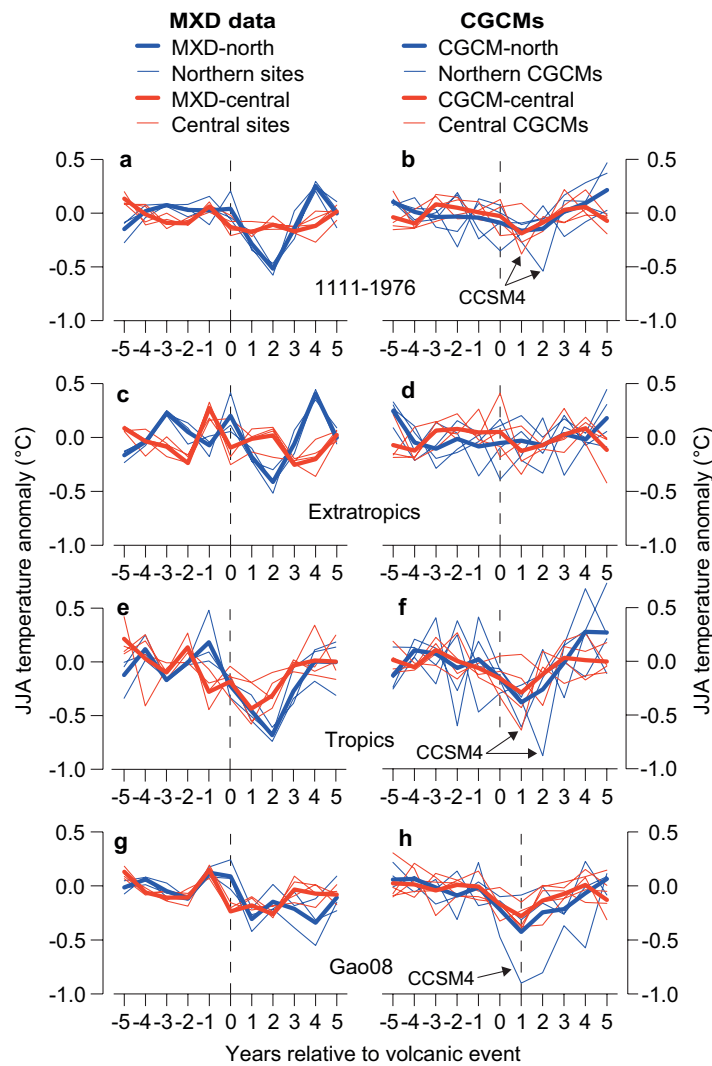
102



104

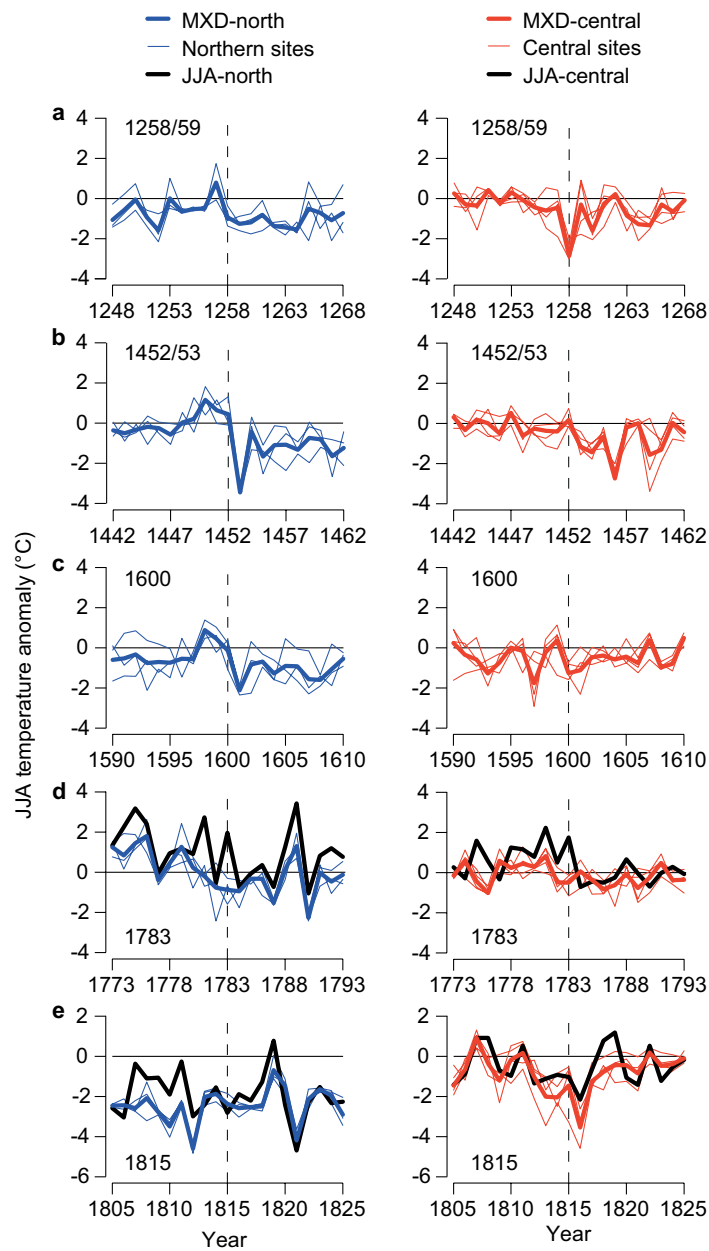
105 **Fig. S4** Superposed Epoch Analyses (SEA) centered on documented and ice core reconstructed
 106 volcanic events. **a** JJA temperature patterns of MXD-north (blue) and MXD-central (red) five years
 107 before and after 22, very large volcanic eruptions (tephra volume $\geq 1.5 \cdot 10^9 \text{ m}^3$) between 1111-1976
 108 C.E. (SEA3 in Table 1). Thin curves are the SEA timeseries of the individual MXD site records JAE,
 109 TOR, and NSC in Northern Europe, and PYR, LAU, LOE, and TIR in Central Europe. **b** Same as in **a**,
 110 but for the 12 eruptions with tephra volumes $1-1.5 \cdot 10^9 \text{ m}^3$ over the same period (SEA4). **c**, Same as in
 111 **a**, but for the 40 Northern Hemispheric volcanic events derived from sulfate depositions in ice cores
 112 over the 1111-1976 period (Gao et al., 2008; SEA7). **d** Same as in **a**, but the 31 volcanic events used
 113 in Briffa et al. (1998) over the 1400-1976 period. Black curve is the MXD-based JJA temperature
 114 reconstruction from Briffa et al. (1998) representing a large fraction of the Northern Hemisphere
 115 (scale on the right axis). **e** Same as in **d**, but for the 11 volcanic events between 1400-1976 that meet
 116 the criteria of **a** (VEI index ≥ 5 , annually dated) and not used in Briffa et al. (1998). All SEA
 117 timeseries expressed as temperature anomalies with respect to the five years preceding volcanic events
 118 (lags -5 to -1). The temperature scale of the Briffa98 and non-Briffa98 SEAs is on the right-hand axes
 119 of panels **d** and **e**

120



122

123 **Fig. S5** SEA centered on documented and ice core derived volcanic eruptions. Left column shows
 124 results for MXD reconstructed JJA temperatures, right column shows results for CGCM JJA
 125 temperatures. **a** and **b** Temperature patterns in Northern (blue) and Central Europe (red) five years
 126 before and after 34 annually dated volcanic eruptions (VEI index ≥ 1.5) over the 1111-1976 C.E.
 127 period (SEA1 in Table 2). Thin curves are the SEA timeseries of the individual MXD site records
 128 (JAE, TOR, NSC in the North; PYR, LAU, LOE, TIR in Central Europe) and the long CGCM runs
 129 (ERIC1, ERIC2, MPI-ESM-P, and CCSM4). The simulations average temperature patterns of five
 130 grid points in proximity to the MXD and instrumental sites in Northern Europe, and seven grid points
 131 in proximity to the MXD and instrumental sites in Central Europe (see Table 3). The bold (red and
 132 blue) curves are the arithmetic means of the four CGCMs. **c-f** Same as in **a** and **b**, but for the 21
 133 Extratropics and 13 Tropical stratospheric eruptions over the 1111-1976 C.E. period (SEA5 and SEA6
 134 in Table 1). **g-h** Same as in **a** and **b**, but for the 40 NH eruptions identified by Gao et al. (2008) based
 135 on ice core data. All SEA timeseries expressed as temperature anomalies with respect to the five years
 136 preceding volcanic events (lags -5 to -1)



138

139 **Fig. S6** JJA temperature anomalies (with respect to the 1961-1990 period) recorded in European MXD
 140 and long station records for the **a** 1258/59 (unknown), **b** 1452/53 (Kuwaë), **c** 1600 (Huaynaputina), **d**
 141 1783 (Laki), and **e** 1815 (Tambora) events. The zoom-in plots show the MXD site (thin blue and red
 142 curves) and regional chronologies (thick blue and red curves) together with the JJA-north and JJA-
 143 central temperature timeseries (black, panels **d** and **e**) ten years before and after the volcanic events.

144

145 **References**

- 146 Briffa KR, Jones PD, Schweingruber FH, Osborn TJ (1998) Influence of volcanic eruptions on
147 Northern Hemisphere summer temperature over the past 600 years. *Nature* 393:450–455
- 148 Crowley TJ (2000) Causes of climate change over the past 1000 years. *Science* 289:270–277
- 149 Crowley T, Zielinski G, Vinther B, Udisti R, Kreutz K, Cole-Dai J, Castellano E (2008) Volcanism
150 and the Little Ice Age. *PAGES Newsletter* 16:22–23
- 151 Crowley TJ, Unterman MB (2012) Technical details concerning development of a 1200-yr proxy
152 index for global volcanism. *Earth Syst Sci Data Discuss* 5:1–28
- 153 Fernández-Donado L, et al. (2013) Large-scale temperature response to external forcing in simulations
154 and 50 reconstructions of the last millennium. *Clim Past* 9:393–421
- 155 Gao C, Robock A, Ammann C (2008) Volcanic forcing of climate over the past 1500 years: An
156 improved ice core-based index for climate models. *J Geophys Res* 113 D23111.
157 doi:10.1029/2008JD010239
- 158 Gent PR., et al. (2011) The Community Climate System Model Version 4. *J Climate* 24:4973–4991
- 159 Giorgetta MA, et al. (2013) Climate change from 1850 to 2100 in MPI-ESM simulations for the
160 Coupled Model Intercomparison Project 5. *J Advances Modell Earth Syst*, in review
- 161 Manley G (1974) Central England temperatures: monthly means 1659 to 1973. *Quart J Royal Met Soc*
162 100:389–405
- 163 Moberg A, Bergström H (1997) Homogenization of Swedish temperature data. Part III: The long
164 temperature records from Stockholm and Uppsala. *Int J Climatol* 17:667–699
- 165 Solomon S, Qin D, Manning M, Chen Z, Marquis M, Averyt KB, Tignor M, Miller HL (eds) (2007)
166 Climate change 2007: the physical science basis. Contribution of working group I to the fourth
167 assessment report of the Intergovernmental Panel on Climate Change. Cambridge Univ Press,
168 Cambridge
- 169 Taylor KE, Stouffer RJ, Meehl GA (2012) An overview of CMIP5 and the experimental design. *Bull*
170 *Amer Meteor Soc* 93:485-497
- 171 van den Dool HM, Krijnen HJ, Schuurmans CJE (1978) Average winter temperatures at De Bilt (the
172 Netherlands) 1634-1977. *Clim Change* 1:319–330
- 173 Vose RS, et al. (1992) The Global Historical Climatology Network (GHCN): long term monthly
174 temperature, precipitation, sea level pressure, and station pressure data. Report ORNL/CDIAC-53,
175 NDP-041 (available from Carbon Dioxide Information Analysis Center, Oak Ridge National
176 Laboratory, Oak Ridge, Tennessee, 1992)

177 Zorita E, Gonzalez-Rouco F, von Storch H, Montavez JP, Valero F (2005) Natural and anthropogenic
178 modes of surface temperature variations in the last thousand years. *Geophys Res Lett* 32 L08707.
179 doi:10.1029/2004GL021563